Bid cleavage, cytochrome release and caspase activation in canine coronavirus-induced apoptosis

Luisa de Martino, Gabriella Marfé, Mariangela Longo, Filomena Fiorito, Serena Montagnaro, Valentina Iovane, Nicola Decaro, Ugo Pagnini

Title: Bid cleavage, cytochrome *c* release and caspase activation in canine coronavirus-induced apoptosis

Authors: Luisa De Martino, Gabriella Marfé, Mariangela Longo, Filomena Fiorito, Serena Montagnaro, Valentina Iovane, Nicola Decaro, Ugo Pagnini

PII: S0378-1135(09)00402-7
DOI: doi:10.1016/j.vetmic.2009.09.001
Reference: VETMIC 4558

To appear in: *VETMIC*

Received date: 13-1-2009
Revised date: 6-8-2009
Accepted date: 4-9-2009

Please cite this article as: De Martino, L., Marfé, G., Longo, M., Fiorito, F., Montagnaro, S., Iovane, V., Decaro, N., Pagnini, U., Bid cleavage, cytochrome *c* release and caspase activation in canine coronavirus-induced apoptosis, *Veterinary Microbiology* (2008), doi:10.1016/j.vetmic.2009.09.001

Bid cleavage, cytochrome *c* release and caspase activation in canine coronavirus-induced apoptosis.

Luisa De Martino[a], Gabriella Marfé[b], Mariangela Longo[a], Filomena Fiorito[a*], Serena Montagnaro[a], Valentina Iovane[a], Nicola Decaro[c], Ugo Pagnini[a]

[a]Department of Pathology and Animal Health, Infectious Diseases, Faculty of Veterinary Medicine, University of Naples "Federico II", Via F. Delpino 1, 80137 Naples, Italy

[b]Department of Experimental Medicine and Biochemical Sciences, University of Rome "Tor Vergata", Via Montpellier 1, 00133 Rome, Italy

[c]Department of Animal Health and Well-being, University of Bari, Strada per Casamassima Km 3, 70010 Valenzano, Bari, Italy.

*Corresponding author: Tel.: +39 081 2536178 – fax: +39 081 2536179

E-mail address: filomena.fiorito@unina.it

Abstract

A previous study demonstrated that infection of a canine fibrosarcoma cell line (A-72 cells) by canine coronavirus (CCoV) resulted in apoptosis (Ruggieri et al., 2007). In this study, we investigated the cell death processes during infection and the underlying mechanisms. We found that CCoV-II triggers apoptosis in A-72 cells by activating initiator (caspase-8 and -9) and executioner (caspase-3 and -6) caspases. The proteolytic cleavage of poly(ADP-ribose) polymerases (PARP) confirmed the activation of executioner caspases. Furthermore, CCoV-II infection resulted in truncated bid (tbid) translocation from the cytosolic to the mitochondrial fraction, the cytochrome *c* release from mitochondria, and alterations in the pro- and anti-apoptotic proteins of bcl-2 family. Our data indicated that, in this experimental model, both intrinsic and extrinsic pathways are involved. In addition, we demonstrated that the inhibition of apoptosis by caspase inhibitors did not affect CCoV replication, suggesting that apoptosis does not play a role in facilitating viral release.

Keywords: Canine coronavirus type II; apoptosis; caspases; PARP; bcl-2 family members.

Introduction

Apoptosis is a particular type of cell death that is characterized by distinctive changes in cellular morphology, including cell shrinkage, nuclear condensation, chromatin margination and subsequent degradation that are associated with inter-nucleosomal DNA fragmentation. Apoptosis may be initiated by a wide variety of cellular insults, including death receptor stimulation and cytotoxic compounds. Induction or inhibition of apoptosis is an important feature of many types of viral infection, both in vitro and in vivo (McLean et al., 2008; Hay and Kannourakis, 2002; Barber, 2001; Derfuss and Meinl, 2002; Benedict et al., 2002; Garnett et al., 2006). Despite this fact, the mechanisms of virus-induced apoptosis remain largely unknown.

Canine coronavirus (CCoV), a member of antigenic group 1 of the family *Coronaviridae*, is a single positive-stranded RNA virus responsible for enteric disease in young puppies (Decaro and Buonavoglia, 2008). CCoV, first described in diarrhoeic dogs (Binn et al., 1974), is responsible for diarrhoea, vomiting, dehydration, loss of appetite and occasional death in puppies. Two serotypes of CCoVs were described (Pratelli et al., 2003), CCoV-I and –II, sharing about 90% sequence identity in most of their genome. In the present study, we evaluated the processes implicated in cell death induced by CCoV, in particular of CCoV type II, which is the only CCoV that grows in cell cultures (Pratelli et al., 2004).

An important regulatory event in the apoptotic process is represented by the caspases activation which regulates two major relatively distinct pathways, the extrinsic and intrinsic pathways. The extrinsic pathway is mediated by activation of caspase-8 that is initiated mainly by binding of death receptors to their ligands. The intrinsic pathway involves the release of cytochrome c from mitochondria; subsequently, cytochrome c binds to the adaptor molecule Apaf-1 (apoptotic protease activating factor-1) causing autocleavage of caspase-9 (Adrain et al., 1999). This pathway known also as mitochondrial pathway involves pro and anti-apoptotic members of the proteins bcl-2 family which can be a key to trigger mitochondrial apoptosis (Hildeman et al., 2002). Both pathways, extrinsic and intrinsic, converge at the activation of executioner caspases (caspase-3, -6 and -7), which are responsible for the characteristic morphological changes of apoptosis (Budihardjo et al., 1999; Elmore, 2007). Generally, both death receptor and mitochondrial apoptosis signalling pathways were shown to be implicated in apoptosis induced by viruses. Induction of caspase-dependent apoptosis has been observed during infection by other coronaviruses, including transmissible gastroenteritis coronavirus (Eleouet et al., 1998), avian coronavirus infectious bronchitis virus (Liu et al., 2001), human coronavirus strain 229E (Collins, 2002), and equine coronavirus (Suzuki et al., 2008).

During infection of CCoV, Ruggieri et al. (2007), demonstrated activation of caspase 3. The aim of this study was to provide a better characterization of the pattern of caspase activation following infection with CCoV-II. We showed that CCoV infection results in the activation of the initiator caspases, caspase-8 and -9, and of the effector caspases, caspase-3 and -6. The data demonstrated that both death receptor and mitochondrial pathways can play an essential role in CCoV-induced apoptosis. Furthermore we observed no variation of CCoV release inhibiting apoptosis by caspase inhibitors.

2. Materials and methods

2.1. Cell culture and virus preparation

A canine fibrosarcoma cell line (A-72 cells) was grown and maintained in complete medium consisting of Dulbecco Minimal Essential Medium (D-MEM) supplemented with 2 mM L-glutamine, 1% non essential amino acid, 5% heat-inactivated foetal calf serum (FCS), 100 IU of penicillin, and 100 μg of streptomycin per ml, at 37°C in a 5% CO_2 atmosphere incubator. This cell line was maintained free of mycoplasma and of bovine viral diarrhoea virus. Cells were trypsinized once a week.

CCoV type II strain S/378 (kindly provided by Prof. C. Buonavoglia, Faculty of Veterinary Medicine, University of Bari, Italy) was used for the study. For viral infection A-72 cells at 80 to 90% confluence in complete medium as described above, were incubated with virus. One hour post-infection (p.i.) non internalized virus was removed by washing the cells three times with DMEM, and incubation continued in complete medium. Virus titers were determined by end point dilution tests using 96-well microtitre plates, and are given as 50% tissue culture infective doses ($TCID_{50}$) according to the method of Reed and Muench (1938). Aliquots of CCoV-II were stored at -80°C until used.

2.2. Cell viability and microscopy

Cell viability after CCoV-II infection was monitored by evaluation of mitochondrial suffering through the MTT assay as previously described (Pagnini et al., 2004). Data are presented as a percentage of the control, and results are the mean ± SEM of three experiments performed in triplicate.

To identify apoptotic nuclei, cells uninfected or infected with CCoV-II, were stained with acridine orange (Sigma Chemical Co, St Louis, USA). Briefly, after 1 h of virus adsorption, the

inoculum was removed and fresh medium was added. After 24 and 48 h p.i., cells were washed with D-MEM and in each well were gently added 100 µl of phosphate-buffered saline (PBS) with acridine orange (40 µg/ml). The cells were incubated at room temperature for approximately 2 min in the dark. The preparations were washed with distilled water, covered with glass cover slips, and assessed on the same day using fluorescent microscope (Zeiss, Oberkochen, Germany) with a 460-nm filter. The duration of illumination was limited to 40 seconds per field. Each experiment was repeated at least three times to confirm the reproducibility of the results. Positive controls were obtained using camptothecin as previously described (Fiorito et al., 2008).

2.3. Caspase detection by flow cytometry

Caspase activation detection was performed by using the carboxyfluorescein FLICA Assay kits (B-Bridge International, Inc., CA, USA). Fluorochrome-labeled inhibitors of caspases (FLICA) included in kits were added during the final 1 h. Precisely, the fluorochrome-labeled inhibitors of caspase-3 (FAM-DEVD-FMK), caspase-8 (FAM-LETD-FMK) and caspase-9 (FAM-LEHD-FMK) were dissolved in DMSO following the manufacturer's instructions and then stored at -20°C in the dark until use. Solutions of each FLICA were added to cell cultures ($1x10^6$ cells/ml) at different times post infection; cells were then incubated for 1h at 37°C in a 5% CO_2 atmosphere incubator. After incubation, cells were washed twice with washing buffer, placed on ice and the cell fluorescence was measured within 15 min by a flow cytometer (Parteck Flow Cytometer). The amount of fluorescence detected was directly proportional to the amount of caspase activity. Results of all experiments are reported as mean ± SEM of three experiments.

2.4. Protein extraction and Western blot analysis

Mock-infected and infected cells (MOI 10) were collected at different times p.i. and washed twice in PBS, then the cell pellets were homogenized directly into lysis buffer (50 mM HEPES, 150 mM NaCl, 1 mM EDTA, 1 mM EGTA, 10% glycerol, 1% NP-40, 1 mM phenylmethylsulfonyl fluoride, 1 µg/ml aprotinin, 0.5 mM sodium orthovanadate, and 20 mM sodium pyrophosphate). The lysates were centrifugated at 14,000 x rpm for 10 min. Protein concentrations were determined by the Bradford assay (Bio-Rad, Hercules, CA). Equivalent amounts of proteins were loaded and electrophoresed on SDS-polyacrylamide gels. Subsequently, proteins were transferred to nitrocellulose membranes (Immobilon, Millipore Corp., Bedford, MA). After blocking with Tris-buffered saline-BSA (25 mM Tris (pH 7.4), 200 mM NaCl, and 5% BSA), the membrane was incubated with the following primary antibodies: anti-caspase-6 PAb (dilution 1:1,000) (Cell Signalling), anti-caspase-3 PAb (dilution 1:1,500) (Abcam), anti-caspase-8 PAb (dilution 1:2,000)

(Abcam), anti-caspase-9 PAb (dilution 1:2,000) (Stressgen), anti-bax PAb (1:1,000) (Aviva Systems Biology), anti-bcl-XL PAb (1:1,000) (Abcam), anti-bcl-2 PAb (1:1,000) (Abcam), anti-bid PAb (1:1000) (Abnova Corporation), anti-cytochrome *c* (1:1000) (Abcam), anti-bim PAb (1:1000) (Cell Signaling) and anti-β-actin MAb (dilution 1:7,500) (Cell Signaling). Membranes were then incubated with the horseradish peroxidase-conjugated secondary antibody (dilution 1:1,000) (at room temperature), and the reaction was detected with an enhanced chemiluminescence system (Amersham Life Science). The relative amount of protein expression was quantified using Gel-Doc phosphorimanger and Quantity One software (Bio-Rad) and normalized by the band intensity of *β*-actin.

2.5. Extraction of PARP

Mock infected and infected cells (MOI 10) were washed twice with ice-cold PBS and then once with ice-cold buffer A (100 mM Tris-HCl [pH 7.4], 10 mM $MgSO_4$, 500 mM sucrose, 10 mM PMSF, 0.5 μg of leupeptin per ml, 0.75 μg of pepstatin per ml, and 5 μg of antipain per ml). Cells were permeabilized by incubation on ice for 20 min with buffer B (100 mM Tris-HCl [pH 7.4], 10 mM $MgSO_4$, 500 mM sucrose, 10 mM PMSF, 1% NP-40; 0.25 μg of leupeptin per ml, 0.35 μg of pepstatin per ml, and 50 μg of antipain per ml). PARP was extracted from permeabilized cells by incubation with cold buffer C (200 mM K_2HPO_4, 100 mM Tris-HCl [pH 7.4], 10 mM $MgSO_4$, 500 mM sucrose, 10 mM PMSF, 0.5 μg of leupeptin per ml, 0.75 μg of pepstatin per ml, and 5 μg of antipain per ml) on ice for 20 min. The extract was centrifuged at 2,000 × *g* for 10 min at 4°C, and the supernatant was collected and mixed with 4 volumes of urea loading buffer (62.5 mM Tris-HCl [pH 6.8], 6 M urea, 10% glycerol, 2% SDS, 0.00125% bromophenol blue, and 5% β-mercaptoethanol). The Western blot analysis of PARP was performed, as above reported, using anti-poly(ADP-ribose) polymerase (PARP) antibody with a dilution of 1:5,000 (BD Biosciences). The relative amount of protein expression was quantified using Gel-Doc phosphorimanger and Quantity One software (Bio-Rad) and normalized by the band intensity of *β*-actin.

2.6. Cytosolic and mitochondrial protein extraction

Isolation of mitochondria and cytosolic fractions were carried out using a modified protocol from Kluck et al. [1997]. Mock-infected and infected cells were collected at different times p.i. and washed twice in PBS. The cell pellets were resuspended in lysis buffer (50 mM Tris [pH 7.5], 150 mM $NaCl_2$, 5 mM EGTA, 1 mM $CaCl_2$, 1 mM $MgCl_2$, 1% NP-40, 1 μg/ml leupeptin, 1 μg/ml aprotinin, 1 μM PMSF, and 100 μM Na_3VO_4). Samples were then incubated on ice for 20 minutes and centrifuged at 14,000 rpm for 15 min. Equivalent amounts of proteins were loaded and

electrophoresed on SDS-polyacrylamide gels. The Western blot analysis of cytochrome *c* was performed, as above reported, using anti-cytochrome *c* PAb with a dilution of 1:1,000 (Abcam). The relative amount of protein expression was quantified using Gel-Doc phosphorimanger and Quantity One software (Bio-Rad) and normalized by the band intensity of *β*-actin.

2.7. Inhibition experiments of CCoV-II-induced apoptosis

A-72 cells in 24-well plates, at confluency, were treated with 25 μM of each of the caspase inhibitors Z-VAD-FMK (pan-caspase inhibitor), Z-IETD-FMK (caspase-8-specifc inhibitor), Z-LEDH-FMK (caspase-9-specific inhibitor), Z-DEVD-FMK (caspase-3-specifc inhibitor) (Calbiochem, EMD Biosciences), 2 h prior to infection with CCoV-II at MOI 10.

At 24 h p.i. cell viability was evaluated by MTT assay as above reported, and virus titers recovered from the culture medium were assayed by TCID50 method according to Reed and Muench (1938).

2.8. Statistical analysis

The results are presented as mean ± SEM of three experiments. One-way ANOVA with Turkey's post test was performed using GraphPad InStat Version 3.00 for Windows 95 (GraphPad Software, San Diego, CA, USA). *P* value < 0.05 was considered statistically significant.

Results

3.1. Cell viability and morphological evidence of apoptosis induced in A-72 cells by CCoV-II infection.

Infection of A-72 cells with CCoV-II resulted in cell death in a time-dependent manner, as detected by MTT assay (Fig. 1). This loss of viability was also dependent on the MOI at which the cultures were infected. Moreover, a significant reduction of mitochondrial dehydrogenases activity was already detectable at 8 h p.i. using a MOI 10 ($P<0.05$). A significant decrease ($P<0.01$ and $P<0.001$) in cell number was observed at all examined times post infection independently of the used MOI .

Using a MOI of 10, the typical cytopathic effects (CPE) characterized by cytoplasmic vacuolation, fusion, rounding up, and detachment of infected cells from the cultured plates were first detected in CCoV type II-infected A-72 cells at 24 h p.i. and the extent of CPE gradually increased by 48 h. (Fig. 2).

Cellular morphological changes were also investigated by acridine orange staining using fluorescence microscopy (Fig. 3). Cells at 80% confluence were mock-infected or infected with

CCoV-II at a MOI of 10. At various time p.i., cells were stained and observed. The results demonstrated that apoptotic morphological changes could be detected overall at 48 h p.i., when cells showed chromatin condensation. Thus, it could be seen clearly that the strong apoptotic signs were evident late in the infection. The data were in accordance with the results of flow cytometric assay (data not shown).

3.2. Activation of caspase cascade

To explore the cell death program, first we investigated caspase activation cascades during CCoV-II-induced apoptosis using a MOI of 10 and analyzing the cell lysates at different times p.i. (8, 12, 24 and 48 h). The activity of two initiator caspase-8 (death receptor-mediated) and caspase-9 (mitochondrial-mediated) as well as the downstream effector caspase-3 were measured using fluorochrome-labeled inhibitors of caspases (FLICA) assay kits.

Fig. 4 shows at and after 12 h p.i. a significant increase ($P<0.01$ and $P<0.001$) of caspase-3, -8 and -9 activity in a time-dependent manner in CCoV-II-infected cells. These data suggested that both extrinsic and intrinsic pathways were involved in CCoV-II-induced apoptosis.

For further evidence, we investigated the initiator caspase-8, 9 activation as well as the executioner caspase-3 and -6 by Western blot analysis. A representative blot (Fig. 5a) and the relative densitometric analysis (Fig. 5b) show the involvement of the examined cleaved caspases. As described in Materials and Methods, β-actin was used as an internal loading control. The cleavage of caspase-8 and -9 was detected from 12 h p.i. in CCoV infected cells (Fig. 5a), and such result was in accordance with FLICA analysis. In particular, it was evident a higher expression level of cleaved caspase-8 compared to cleaved caspase-9 at 12 h p.i.. Then, whereas the cleaved caspase-8 showed a time-dependent downward trend, the cleaved caspase-9 didn't change over time.

The caspase-3 activation pattern was also well correlated with the FLICA analysis. In fact, we observed the caspase-3 proteolytic processing at and after 12 h p.i., and a significant peak at 24 and 36 h p.i. (Fig. 5a and b). By Western blot analysis, we have also observed the cleaved caspase-6 (Fig. 5a and b) and a higher activation of caspase-6 at and after 24 h p.i. than that of caspase-3.

3.3. PARP cleavage

We next assessed the cleavage of PARP in the induction of apoptosis in A-72 cells by CCoV-II. PARP is a substrate for activated caspase-3 and cleaved PARP is considered a hallmark of apoptosis (Elmore, 2007). PARP cleavage was monitored during CCoV-II infection by Western blot in order to provide additional evidence of caspase activation and apoptosis induced by CCoV-II. As shown in Fig. 6a, the full-length 116 kDa PARP was cleaved to active form of 85 kDa in

time-dependent manner. A representative blot (Fig. 6a) and its quantification (Fig. 6b) shows the involvement of proteolytic cleavage of PARP in virus-infected cells harvested at 12, 24, 36 and 48 h p.i., when the typical DNA laddering was also evident (data not shown). Furthermore, the Fig. 6c shows that the cleaved PARP/uncleaved PARP ratio was statistically significant ($P<0.01$) from 24 h p.i. until the end of infection compared to that of 12 h p.i..

3.4. Bid cleavage and cytochrome c release

In normal cells, the bid protein exists as an inactive form in the cytosolic fraction and becomes activated by caspase-8 in response to apoptotic stimuli. Then, the active form of bid translocates to the mitochondria, and triggers bax activation in correlation with the translocation of bax from the cytosol to the mitochondria. These events result in the cytochrome *c* release from the mitochondria to the cytosol (Korsmeyer et al., 2000; Roucou et al., 2002). Because CCoV-II infection, as shown above, induced caspase-8 activation in infected cells, we generated subcellular fractions to examine bid and cytochrome *c* cell localization. As shown in Fig. 7a and b, the full-length bid expression level evaluated by Western blot analysis in cytosolic fraction, decreased in time-dependent in virus-infected cells respect to mock-infected cells. The mitochondrial localization of 15 kDa fragment truncated bid (tbid) clearly appeared at 12 h p.i. Since this fragment contains the BH3 domain which is the functional part of bid for cytochrome *c* release, we examined whether the bid traslocation was accompanied by a mitochondrial release of cytochrome *c* into the cytosol. The relationships with bid-induced cytochrome *c* release is evident in Fig. 7c and d which shows the presence of cytochrome *c* in the cytosolic fraction from 12 h p.i. until the end of infection.

3.5. Effect of CCoV type II infection on the expression of Bcl-2 family of proteins

The Bcl-2 family of proteins, including both inhibitors and promoters of apoptosis, is involved in the controlling of mitochondrial permeability, as well as regulation of caspase activation. In this study, several Bcl-2 family proteins, including anti-apoptotic (bcl-2, bcl-xL) and pro-apoptotic members (bax, bim), were detected in response to CCoV-II infection in A-72 cells. The densitometric analysis of the blots demonstrated an increased expression of pro-apoptotic proteins, bim and bax, which presented a peak at 12 and 24 h p.i. respectively; but while the levels of bim protein slightly decreased after 36 h p.i., bax levels didn't change (Fig. 8a and b). Whereas the expressions of the anti-apoptotic members, bcl-2 and bcl-xL, were downregulated by CCoV-II infection (Fig. 8a). The densitometric analysis of the blots demonstrated a decreased expression of

bcl-2 and of bcl-xL after 8 h and 12 h p.i. respectively (Fig. 8b). The data suggest that bax, bim, bcl-2 and bcl-xL may play a role on arbitrating the CCoV type II-induced apoptosis.

3.2- *Effects of caspase inhibitors on cell viability and viral replication*

To test if the apoptotic changes observed in CCoV type II-infected A-72 cells were caspase dependent, Z-VAD-FMK (pan-caspase inhibitor), Z-DEVD-FMK (caspase-3-specific inhibitor), Z-IETD-FMK (caspase-8-specific inhibitor), Z-LEHD-FMK (caspase-9 inhibitor) were added to the culture media before the infection. As shown in Fig. 9a, in presence of caspases inhibitors was observed a significant higher cell viability ($P<0.001$).

The effects of apoptosis on the replication of CCoV-II were assayed by comparing virus titers in the presence of caspase inhibitors. As reported in Fig. 9b, the results showed that the virus release in presence of caspase inhibitors didn't change compared with control. It is conceivable that apoptosis is not required for the release of progeny virions. These observations therefore suggest that CCoV-II replication don't requires caspase activation to complete the virus life cycle.

Discussion

It is believed that the modulation of apoptotic cell death, also known as programmed cell death, is relevant to diseases that are caused by various viruses. One of the main advantages of apoptotic cell death for virus infectivity is to facilitate the spread of virus progeny to the neighboring cells and to minimize the inflammatory reaction evoked by virus-infected cells on the host.

Coronaviruses are known to infect host cells by receptor-mediated endocytosis and some of them to cause cell-cell fusion during the late stages of infection, resulting in synctium formation and CPE (Lai and Cavanagh, 1997). Apoptosis was observed in Vero E6 cells infected by SARS-CoV (Yan et al., 2004) and in a recent publication it has been reported that CCoV induces apoptosis in cultured cells (Ruggieri et al., 2007). It has been shown that in other coronavirus, e.g., avian infectious bronchitis virus (Liu et al., 2001), swine transmissible gastroenteritis virus (Eleouet et al., 2000) and murine coronavirus (Liu et al., 2006; Liu and Zhang, 2007), apoptosis is induced by a caspase-dependent mechanism.

The importance of caspase activation during apoptosis is well established (Hengartner, 2000). Caspases play a central role in the effector phase during apoptotic cell death. To date, 14 mammalian caspases have been described (Earnshaw et al., 1999).

In this study we show that CCoV type II infection leads to caspase-dependent apoptotic cell death in A-72 cells, *in vitro*. First, we examined by MTT assay and morphological evaluations the CCoV-II infection, demonstrating a dose- and time-dependent trend of the apoptotic process virus-induced. Then, in an attempt to understand the mechanism of induction of apoptosis in CCoV-II-infected cells we have investigated the caspase pathways. The results reported herein by FLICA method (Bedner et al., 2000) provide an unequivocal evidence that CCoV-II induces apoptotic cell death *in vitro*, involving caspase-dependent pathway of caspase-8 (death receptor-mediated) and caspase-9 (mitochondrial-mediated). This suggests that both the extrinsic and intrinsic pathways in the CCoV-II-induced apoptosis were involved. Our results match those Eleouet et al. (2000) who demonstrated that the transmissible gastroenteritis coronavirus (TGEV), also included in group 1 coronaviruses as CCoV-II, triggers caspase activation events, involving both the extrinsic and intrinsic pathways, during infection. Further apoptosis-associated caspase activation has been documented also in other coronavirus groups such as SARS CoV (group 2) (Mizutani et al., 2004), MHV (group 2) (Chen and Makino, 2002), and IBV (group 3) (Liu et al, 2001).

However, in the present study, it was evident the activation of caspase-8 and -9 at and after 12 h p.i. by FLICA and Western blot analysis. Furthermore, caspase 9 was only partially activated compared to the others investigated and not changing between times 24 -72 hours suggesting that viral proteins could interfere with such activation. A higher protein expression level of caspase-3 and -6 compared to those of caspase-8 and -9, after 12 h p.i., was observed. These higher levels of activity achieved by caspase-3 and -6 could be related to the additive effect of both caspase-8 and -9 pathways that activate these executioner caspases.

Caspase-8 has been shown to activate the intrinsic pathway following the cleavage of bid, a pro-apoptotic member of the Bcl-2 family of proteins (Li et al., 1998). The data herein presented are consistent with such mechanism, showing that the full-length bid expression level in cytosolic fraction decreased in time-dependent in virus-infected cells respect to mock-infected cells. We also described the relationships with bid-induced cytochrome *c* release in the cytosolic fraction from 12 h p.i. until the end of infection.

Bid is part of the bcl-2 family of proteins, which includes both pro-apoptotic proteins (for example bid, bax, bak, bcl-XS, bad, bim), and anti-apoptotic proteins (for example bcl-2, bcl-XL bcl-w, mcl-1). Therefore, the bcl-2 family of proteins have been considered as pivotal players in apoptosis. Our study has shown that CCoV-II infection down-regulated bcl-2 but up-regulated bax expression. Furthermore, densitometric analysis of bim, which is one of the candidates for initial mitochondrial activation, indicated a marked increase of protein expression level up to 36 h p.i.. Bim activates bax through interactions with mcl-1 and bcl-2 (Willis et al., 2007). Here we have

reported that bim significantly shifted the relative contributions of bax to cell death. Then, in response to apoptotic stimuli, bax has to translocate to mitochondria before it can oligomerize and form pores (Desagher and Martinou, 2000), and the relative decline in bcl-2 expression permits bax to gain dominance, the downstream effects of which most likely involve both direct and indirect activation of the cell death proteases that represent the final steps in the apoptotic pathway.

We have also shown additional evidence of downstream caspase activation evaluating the PARP cleavage during CCoV-II infection. PARP is a substrate for activated caspase-3 (Li and Darzynkiewicz, 2000), and here we have shown elevated expression of activated caspase-3 and cleaved PARP in the CCoV-II-infected cells in time–dependent manner. Thus, the CCoV-II-infection significantly increased PARP cleavage levels.

Furthermore, we observed the effects of apoptosis on both the replication of CCoV type II and virus titers in the presence of caspase inhibitors. The suppression of apoptosis by these inhibitors suggested that the activation of apoptosis doesn't represent an important step in virus release. These data are in agreement with previous studies, in fact, it was demonstrated that the inhibition of apoptosis, either by caspase inhibitors or by overexpression of the bcl-2 protein, did not affect SARS-CoV replication in Vero cells (Ren et al., 2005; Bordi et al., 2006), suggesting that apoptosis does not play a role in facilitating viral release.

Collectively, the results reported here demonstrate that: (i) apoptosis developing in a CCoV-II infection depended on the activition of caspase-3,-6 -8 and -9; (ii) apoptosis induced during *in vitro* infection of A-72 cells could occur both from the extrinsic pathway and the intrinsic pathway; (iii) CPE and cell death in A-72 cells, which are triggered by CCoV-II, are due to the induction of caspase activation, given the ability of caspase inihibitors to increase viability of CCoV-II-infected cell; and (iv) there is no interference between apoptosis and viral release.

These results suggest that this coordinated interplay among caspases is crucial in attaining full activation of apoptotic signal in A-72 infected cells; however, the first direct link between caspase activation and CCoV-II-induced apoptosis remains to be explored and studies are under way in order to identify targets of viral protein involved in the modulation of apoptosis during CCoV-II-infection.

382 **References**

383

384 Adrain, C., Slee, E.A., Harte, M.T., Martin, S.J., 1999. Regulation of apoptotic protease
385 activating factor-1 oligomerization and apoptosis by the WD-40 repeat region. J. Biol.
386 Chem. 274, 20855-20860.
387 Barber, G.N., 2001. Host defense, viruses and apoptosis. Cell Death Differ. 8, 113-126.
388 Bedner, E., Smolewski, P., Amstad, P., Darzynkiewicz, Z., 2000. Activation of caspases
389 measured in situ by binding of fluorochrome-labeled inhibitors of caspases (FLICA):
390 correlation with DNA fragmentation. Exp. Cell Res. 259, 308-313.
391 Benedict, C.A., Norris, P.S., Ware, C.F., 2002. To kill or be killed: viral evasion of apoptosis.
392 Nat. Immunol. 3, 1013–1017.
393 Binn, L.N., Lazar, E.C., Keenan, K.P., Huxoll, D.L., Marchwicki, R.H., Strano, A.J., 1974.
394 Recovery and characterization of a coronavirus from military dogs with diarrhoea. Proc.
395 Annu. Mtg US Anim. Health Assoc. 78, 359–366.
396 Bordi, L., Castilletti, C., Falasca, L., Ciccosanti, F., Calcaterra, S., Rozera, G., Di Caro, A.,
397 Zaniratti, S., Rinaldi, A., Ippolito, G., Piacentini, M., Capobianchi, M.R., 2006. Bcl-2
398 inhibits the caspase-dependent apoptosis induced by SARS-CoV without affecting virus
399 replication kinetics. Arch. Virol. 151, 369–377.
400 Budihardjo, I., Oliver, H., Lutter, M., Luo, X., Wang, X., 1999. Biochemical pathways of
401 caspase activation during apoptosis. Annu. Rev. Cell Dev. Biol. 15, 269-290.
402 Chen, C.J., Makino, S., 2002. Murine coronavirus-induced apoptosis in 17Cl-1 cells involves a
403 mitochondria-mediated pathway and its downstream caspase-8 activation and bid cleavage.
404 Virology 302, 321-332.
405 Collins, A.R., 2002. In vitro detection of apoptosis in monocytes/macrophages infected with
406 human coronavirus. Clin. Diagn. Lab. Immunol. 9, 1392-1395.
407 Decaro, N., Buonavoglia, C., 2008. An update on canine coronaviruses: Viral evolution and
408 pathobiology. Vet. Microbiol. 132, 221-234.
409 Derfuss, T., Meinl, E., 2002. Herpesviral proteins regulating apoptosis. Curr. Top. Microbiol.
410 Immunol. 269, 257-272.
411 Desagher, S., Martinou, J.C., 2000. Mitochondria as the central control point of apoptosis.
412 Trends Cell Biol. 10, 369-377.
413 Earnshaw, W.C., Martins, L.M., Kaufmann, S.H., 1999. Mammalian caspases : structure,
414 activation, substrates, and functions during apoptosis. Ann. Rev. Biochem. 68, 383-424.

Eleouet, J.F., Chilmonczyk, S., Besnardeau, L., Laude, H., 1998. Transmissible gastroenteritis coronavirus induces programmed cell death in infected cells through a caspase-dependent pathway. J. Virol. 72, 4918-4924.

Eleouet, J.F., Slee, E.A., Saurini, F., Castagne, N., Poncet, D., Garrido, C., Solary, E., Martin, S.J., 2000. The viral nucleocapsid protein of transmissible gastroenteritis coronavirus (TGEV) is cleaved by caspase-6 and -7 during TGEV-induced apoptosis. J. Virol. 74, 3975-3983.

Elmore, S., 2007. Apoptosis: a review of programmed cell death. Toxicol. Pathol. 35, 495-516.

Fiorito, F., Pagnini, U., De Martino, L., Montagnaro, S., Ciarcia, R., Florio, S., Pacilio, M., Fucito, A., Rossi, A., Iovane, G., Giordano, A., 2008. 2,3,7,8-Tetrachlorodibenzo-p-dioxin increases Bovine Herpesvirus type-1 (BHV-1) replication in Madin-Darby bovine kidney (MDBK) cells in vitro. J. Cell. Biochem. 103, 221–233.

Garnett, T.O., Filippova, M., Duerksen-Hughes, P.J., 2006. Accelerated degradation of FADD and procaspase 8 in cells expressing human papilloma virus 16 E6 impairs TRAIL-mediated apoptosis. Cell Death Differ. 13, 1915-1926.

Hay, S., Kannourakis, G., 2002. A time to kill: viral manipulation of the cell death program. J. Gen. Virol. 83, 1547-1564.

Hengartner, M.O., 2000. The biochemistry of apoptosis. Nature 407, 770-776.

Hildeman, D.A., Zhu, Y., Mitchell, T.C., Bouillet, P., Strasser, A., Kappler, J., Marrack, P., 2002. Activated T cell death in vivo mediated by proapoptotic bcl-2 family member bim. Immunity 16, 759-767.

Kluck, R.M., Bossy-Wetzel, E., Green, D.R., Newmeyer, D.D., 1997. The release of cytochrome c from mitochondria: a primary site for Bcl-2 regulation of apoptosis. Science 275, 1132-1136.

Korsmeyer, S.J., Wei, M.C., Saito, M., Weiler, S., Oh, K.J., Schlesinger, P.H., 2000. Pro-apoptotic cascade activates BID, which oligomerizes BAK or BAX into pores that result in the release of cytochrome c. Cell Death Differ. 7, 1166-1173.

Lai, M.M.C., Cavanagh, D., 1997. The molecular biology of coronaviruses. Adv. Virus Res. 48, 1-100.

Li, H., Zhu, H., Xu, C. J., Yuan. J., 1998. Cleavage of BID by caspase 8 mediates the mitochondrial damage in the Fas pathway of apoptosis. Cell 94**,** 491–501.

Li, X., Darzynkiewicz, Z., 2000. Cleavage of Poly(ADP-ribose) polymerase measured in situ in individual cells: relationship to DNA fragmentation and cell cycle position during apoptosis. Exp. Cell Res. 255, 125-132.

449 Liu, C., Xu, H.Y., Liu, D.X., 2001. Induction of caspase-dependent apoptosis in cultured cells
450 by the avian coronavirus infectious bronchitis virus. J. Virol. 75, 6402-6409.
451 Liu, Y., Pu, Y., Zhang, X., 2006. Role of the mitochondrial signaling pathway in murine
452 coronavirus-induced oligodendrocyte apoptosis. J. Virol. 80, 395-403.
453 Liu, Y., Zhang, X., 2007. Murine coronavirus-induced oligodendrocyte apoptosis is mediated
454 through the activation of the Fas signalling pathway. Virology 360, 364-375.
455 McLean, J.E., Ruck, A., Shirazian, A., Pooyaei-Mehr, F., Zakeri, Z.F., 2008. Viral manipulation
456 of cell death. Curr. Pharm. Des. 14, 198-220.
457 Mizutani, T., Fukushi, S., Saijo, M., Kurane, I., Morikawa, S., 2004. Phosphorylation of p38
458 MAPK and its downstream target in SARS coronavirus-infected cells. Biochem. Biophys.
459 Res. Commun. 319, 1228-1234.
460 O'Brien, V., 1998. Viruses and apoptosis. J. Gen. Virol. 79, 1833-1845.
461 Pagnini, U., Montagnaro, S., Pacelli, F., De Martino, L., Florio, S., Rocco, D., Iovane, G.,
462 Pacilio, M., Gabellino, C., Marsili, S., Giordano, A.. 2004. The involvement of oxidative
463 stress in bovine herpesvirus type 4-mediated apoptosis. Front. Biosci, 9, 2106–2114.
464 Pratelli, A., Decaro, N., Tinelli, A., Martella, V., Elia, G., Tempesta, M., Cirone, F.,
465 Buonavoglia, C., 2004. Two genotypes of canine coronavirus simultaneously detected in the
466 fecal samples of dogs with diarrea. J. Clin. Microbiol. 42, 1797-1799.
467 Pratelli, A., Martella, V., Decaro, N., Tinelli, A., Camero, M., Cirone, F., Elia, G., Cavalli, A.,
468 Corrente, M., Greco, G., Buonavoglia, D., Gentile, M., Tempesta, M., Buonavoglia, C.,
469 2003. Genetic diversity of a canine coronavirus detected in pups with diarrhoea in Italy. J.
470 Virol. Methods 110, 9-17.
471 Reed, L.J., Muench, H., 1938. A simple method of estimating 50 per cent end-points. Am. J.
472 Hyg. 27, 493-497.
473 Ren, L., Yang, R., Guo, L., Qu, J., Wang J., Hung, T., 2005. Apoptosis induced by the SARS-
474 associated coronavirus in Vero cells is replication-dependent and involves caspase. DNA
475 Cell Biol. 24, 496–502.
476 Roucou, X., Montessuit, S., Antonsson, B., Martinou, J.C., 2002. Bax oligomerization in
477 mitochondrial membranes requires tBid (caspase-8-cleaved Bid) and a mitochondrial
478 protein. Biochem. J. 15, 915-921.
479 Ruggieri, A., Di Trani, L., Gatto, I., Franco, M., Vignolo, E., Bedini, B., Elia, G., Buonavoglia,
480 C., 2007. Canine coronavirus induces apoptosis in cultured cells. Vet. Microbiol.121, 64-72.
481 Ruggieri, A., Harada, T., Matsuura, Y., Miyamura, T., 1997. Sensitization to Fas-mediated
482 apoptosis by hepatitis C virus core protein. Virology 229, 68-76.

483 Shen, Y., Shenk, T.E., 1995. Viruses and apoptosis. Curr. Opin. Genet. Dev. 5, 105-111.
484 Suzuki, K., Matsui, Y., Miura, Y., Sentsui, H., 2008. Equine coronavirus induces apoptosis in
485 cultured cells. Vet. Microbiol. 129, 390-395.
486 Willis, S.N., Fletcher, J.I., Kaufmann, T., van Delft, M.F., Chen, L., Czabotar, P.E., Ierino, H.,
487 Lee, E.F., Douglas Fairlie, W., Bouillet, P., Strasser, A., Kluck, R.M., Adams, J.M.,
488 Huang, D.C.S., 2007. Apoptosis initiated when BH3 ligands engage multiple Bcl-2
489 homologs, not Bax or Bak. Science 315, 856-859.
490 Yan, H., Xiao, G., Zhang, J., Hu, Y., Yuan, F., Cole, D.K., Zheng, C., Gao, G.F., 2004. SARS
491 coronavirus induces apoptosis in Vero E6 cells. J. Med. Virol. 73, 323-331.
492

Legends

Fig. 1 – Effect of various MOI of CCoV-II on A-72 cell viability. After the indicated times of post infection, cell viability was evaluated with MTT assay. Values represent the mean (±SEM) of three different experiments performed in triplicate. *p < 0.05, ** p < 0.01, *** p < 0.001 compared to mock-infected cultures.

Fig. 2 – Photomicrographs at inverted microscope of CCoV-II-induced cytopathic effect (CPE) using a MOI of 10, **A**, mock-infected A-72 cells; **B**, CCoV-II –infected cells at 24 h p.i.; **C**, CCoV-II –infected cells at 48 h p.i.. Magnification: 100x..

Fig. 3 – Photomicrographs under fluorescence microscopy showing morphological changes in CCoV-II-infected cells (MOI 10) after orange acridine staining. **A,** mock-infected cells**; B,** CCoV-II -infected cells at 24 h p.i.; **C,** CCoV-II –infected cells at 48 h p.i.. Magnification: 400x.

Fig. 4 – Caspase-3, -8 and -9 activation by flow cytometric analysis. Caspase-3 FLICA (FAM-DEVD-FMK), caspase-8 FLICA (FAM-LETD-FMK) and caspase-9 FLICA (FAM-LEHD-FMK) was added at the last hour of treatment to evaluate their activation. The results of fluorescence profiles of CCoV-II-infected cells (MOI 10) at 8, 12, 24 and 48 h p.i. are reported. The data are presented as the means ± SEM of the results of three separate experiments. Significant differences between CCoV-II infected group and mock-infected groups are indicated by probability P. **P<0.01, and ***P<0.001.

Fig. 5 – Effects of CCoV-II infection on the caspase cascade activation. **a)** Western blot analysis of cleaved caspase-8, -9, -6 and -3 in CCoV-II-infected cells (MOI 10). Cells were mock-infected (lane cc) and CCoV-II infected for the indicated times (4, 8, 12, 24, 36 and 48 h p.i.). Cellular extracts were analysed by Western blot using anti-caspase-8, -9, -6 and 3 antibodies. *β*-actin was used as an internal loading control. The molecular weight (kDa) of protein size standards is shown on the left hand side. Blot is representative of three separate experiments. **b)** Densitometric analysis of blots relative to cleaved caspase-8, -9, -6 and -3. Results are expressed as the mean ± SEM of three separate experiments.

Fig. 6 - Western blot analysis of PARP activation in CCoV-II-infected cells (MOI 10). **a)** Cells were mock-infected (lane cc) and CCoV-II infected cells (4, 8, 12, 24, 36, and 48 h p.i.). Cellular extracts were analyzed by Western blot using specific antibody. *β*-actin was used as an internal

528 loading control. The molecular weight (kDa) of protein size standards is shown on the left hand
529 side. Blot is representative of three separate experiments. **b)** Densitometric analysis of blots relative
530 to cleaved and uncleaved PARP. Results are expressed as the mean ± SEM of three separate
531 experiments. **c)** Cleaved PARP/uncleaved PARP ratio in infected-cells obtained by densitometric
532 analysis. Significant difference between the value at 12 h p.i. and the others times of p.i. are
533 indicated by probability *P*. **P < 0.01.
534
535 **Fig. 7** – Western blot analysis of bid and cytochrome *c* in CCoV-II-infected cells (MOI 10). **a)** Bid
536 cleavage and translocation of tbid to mitochondria. The cells were mock-infected (lane cc) and
537 CCoV-II infected (4, 8, 12, 24, 36 and 48 h p.i.). Cell lysates were collected at the indicated times
538 p.i., and equal amounts of protein from each sample were subjected to Western blot analysis. *β*-
539 actin was used as an internal loading control. The molecular weight (kDa) of protein size standards
540 is shown on the left hand side. Blot is representative of three separate experiments. **b)**
541 Densitometric analysis of blots relative to bid. Results are expressed as the mean ± SEM of three
542 separate experiments. **c)** Cytochrome *c* release in cytosol fraction. Cell lysates were collected at the
543 indicated times p.i., and equal amounts of protein from each sample were subjected to Western blot
544 analysis, and probed for cytochrome *c*. *β*-actin was used as an internal loading control. The
545 molecular weight (kDa) of protein size standards is shown on the left hand side. Blot is
546 representative of three separate experiments. **d)** Densitometric analysis of blots relative to
547 cytochrome *c*. Results are expressed as the mean ± SEM of three separate experiments.
548
549 **Fig. 8** - Effects of CCoV-II infection (MOI 10) on bcl-2 family proteins. **a**) Analysis of bax, bim,
550 bcl-2 and bcl-XL proteins expression. Whole-cell lysate was prepared from mock infected (lanes
551 cc) and infected cells at the indicated times (4, 8, 12, 24, 36 and 48 h p.i.). Western blot analysis
552 was performed with an antibody which specifically recognized bax, bim, bcl-2 and bcl-XL and β-
553 actin. *β*-actin was used as an internal loading control. The molecular weight (kDa) of protein size
554 standards is shown on the left hand side. Blot is representative of three separate experiments. **b)**
555 Densitometric analysis of blots relative to bcl-2 family proteins. Results are expressed as the mean
556 ± SEM of three separate experiments.
557
558 **Fig. 9** - Effect of caspase inhibitors on cell viability and virus release in CCoV-II-infected cells
559 (MOI 10). **a)** A-72 cells were treated with Z-VAD-FMK (pan-caspase inhibitor), Z-DEVD-FMK
560 (caspase-3-specific inhibitor), Z-IETD-FMK (caspase-8-specific inhibitor), Z-LEHD-FMK
561 (caspase-9 inhibitor) 1 h prior to infection with CCoV-II. The cell viability were analyzed at 24 h

562 after infection by MTT assay. Data are presented as a percentage of the untreated cell control, and
563 the results are the mean ± SEM of three independent experiments. ***P < 0.001. **b)** Virus titration.
564 The titer of virus released from cells treated with caspase inhibitors was estimated by $TCID_{50}$. Data
565 are presented as the mean ± SEM of three separate experiments.
566

Figure 1

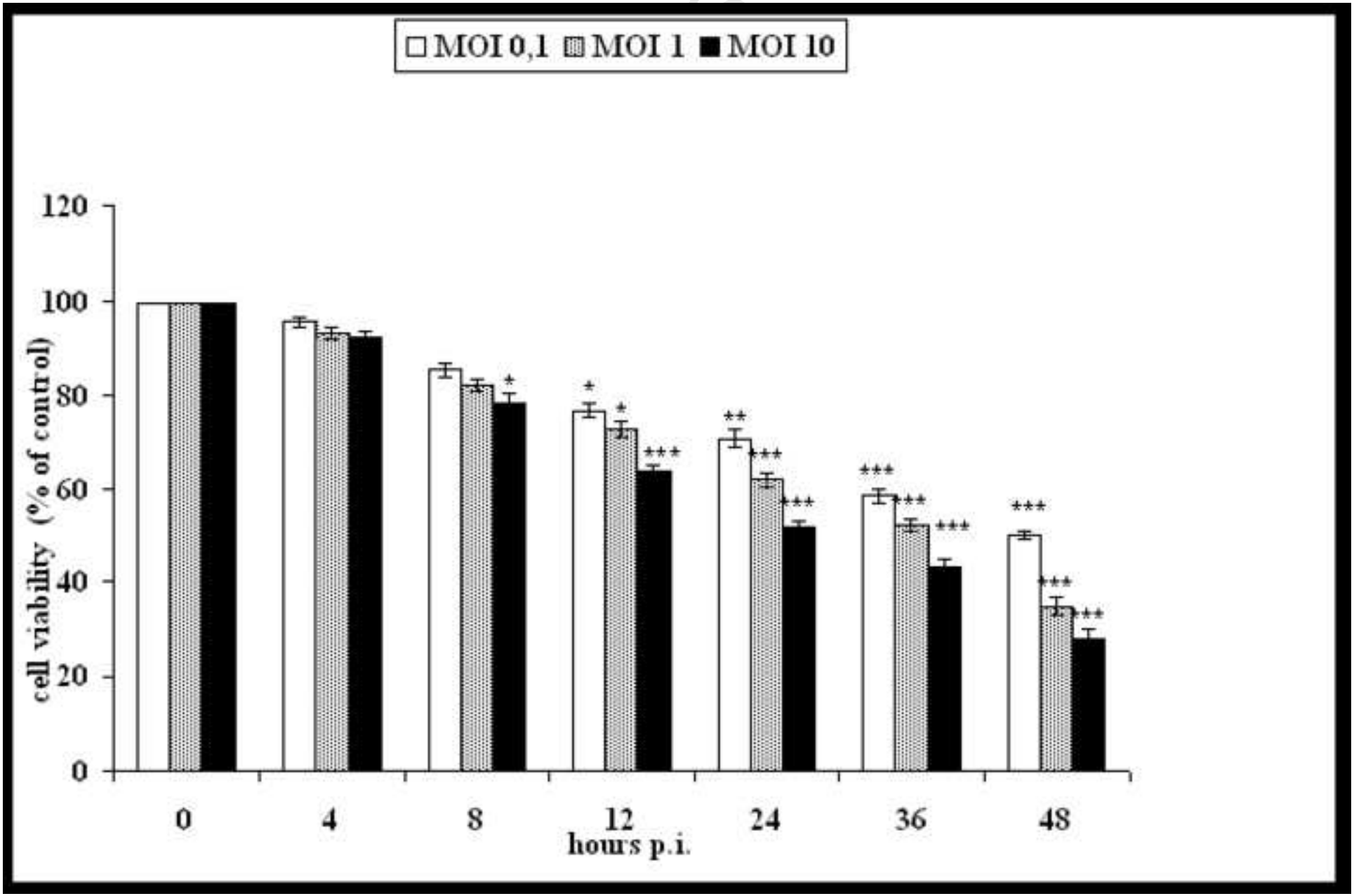
MOI 0,1
MOI 1
MOI 10
cell viability (% of control)
120
100
80
60
40
20
0
0
4
8
12
24
36
48
hours p.i.

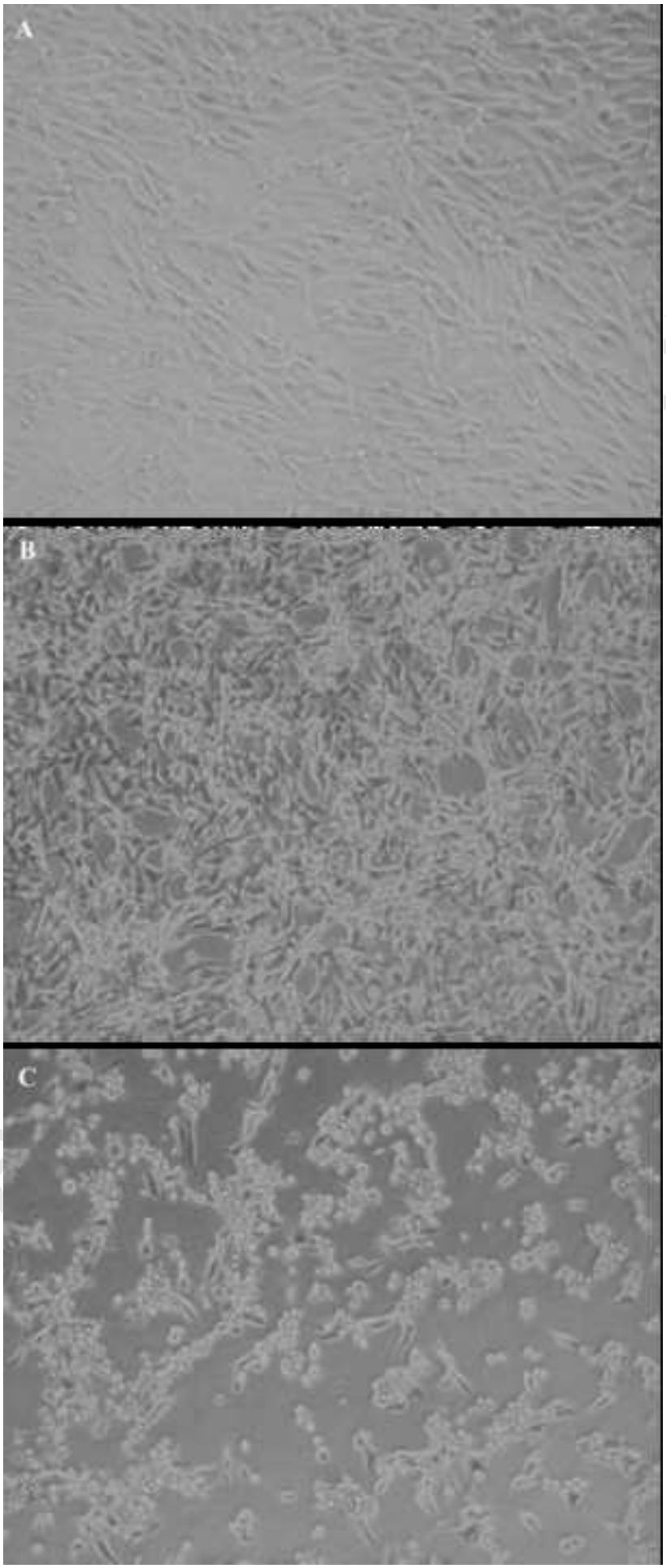

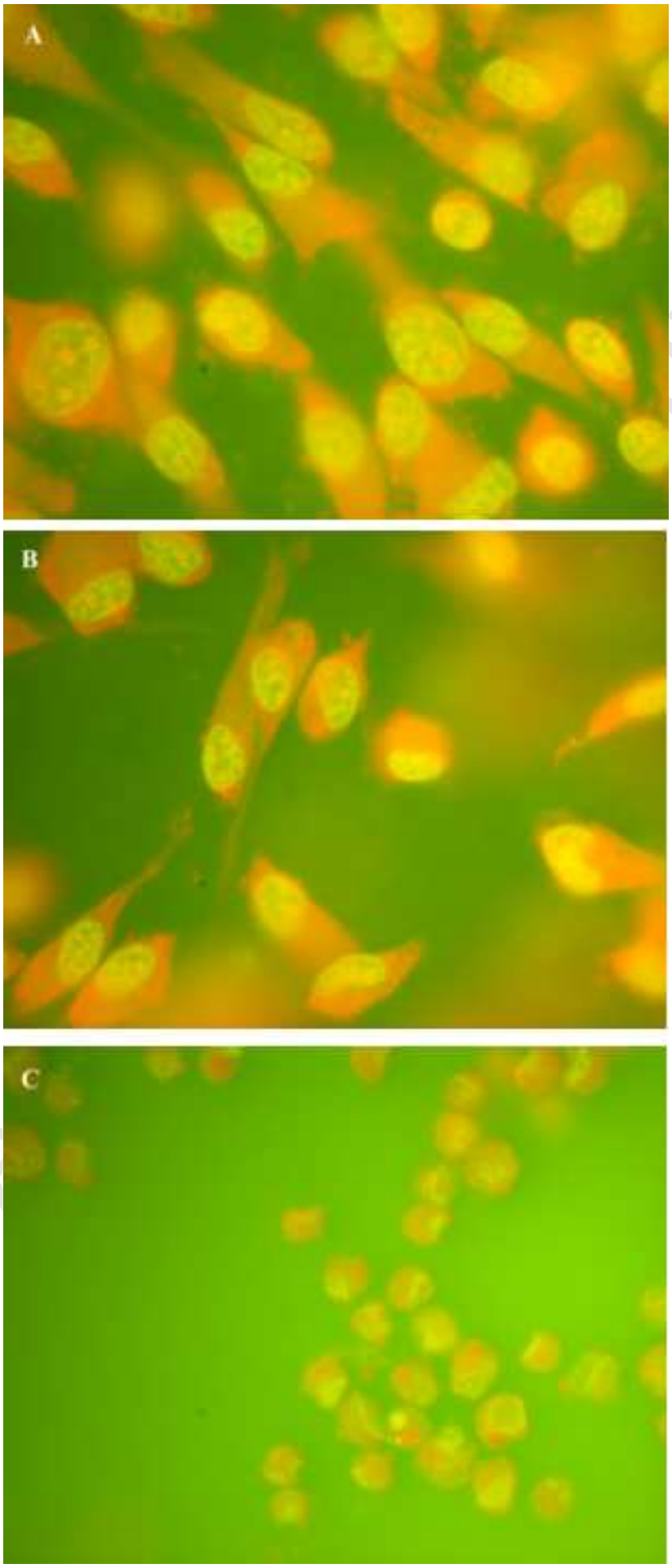

Figure 4

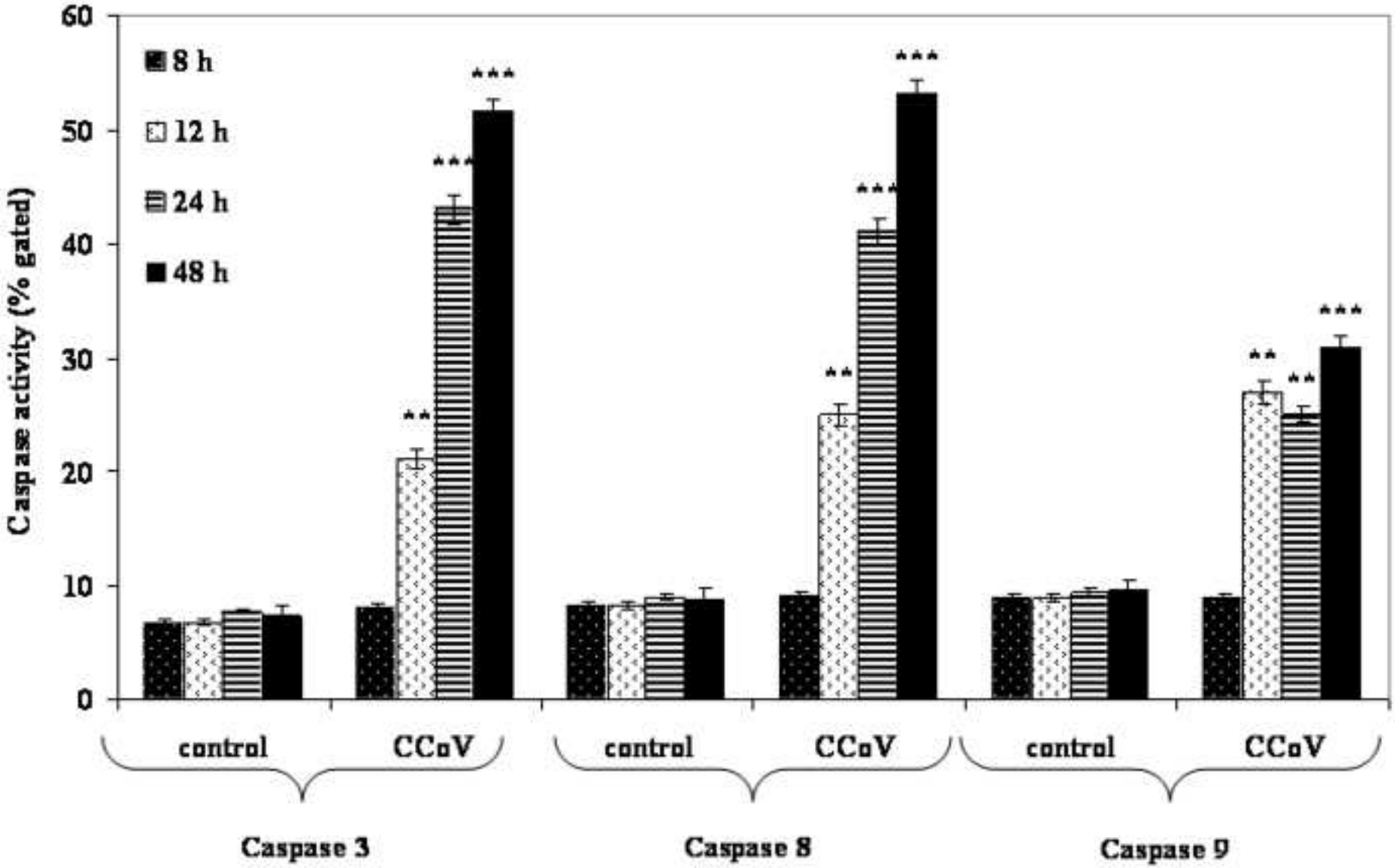
60
50
40
30
20
10
0
Caspase activity (% gated)
8 h
12 h
24 h
48 h
**
***
***
**
***
***
**
**
***
control
CCoV
control
CCoV
control
CCoV
Caspase 3
Caspase 8
Caspase 9

Figure 5

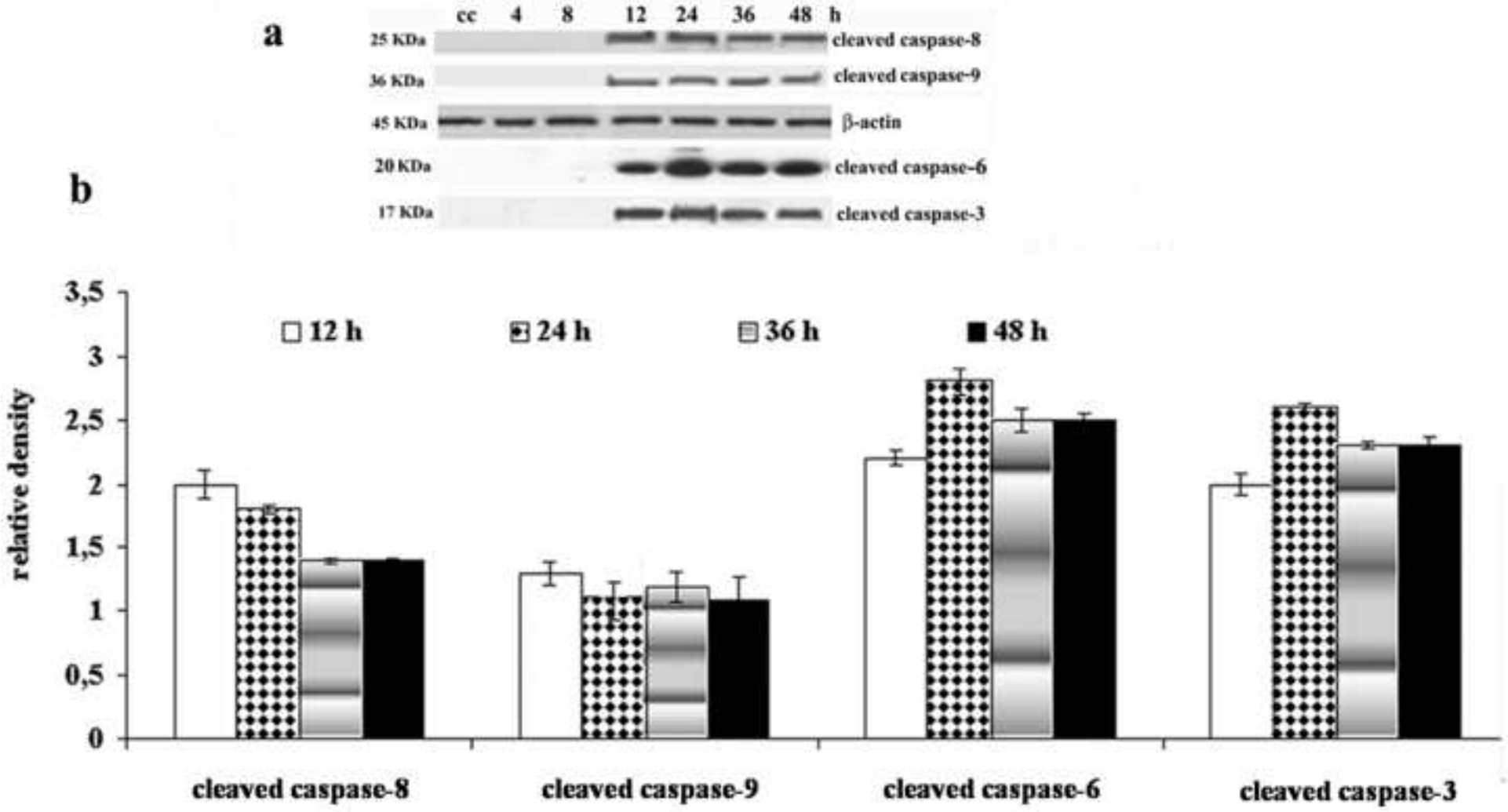
a
cc 4 8 12 24 36 48 h
25 KDa
cleaved caspase-8
36 KDa
cleaved caspase-9
45 KDa
β-actin
20 KDa
cleaved caspase-6
17 KDa
cleaved caspase-3
b
12 h
24 h
36 h
48 h
relative density
3,5
3
2,5
2
1,5
1
0,5
0
cleaved caspase-8
cleaved caspase-9
cleaved caspase-6
cleaved caspase-3

Figure 6

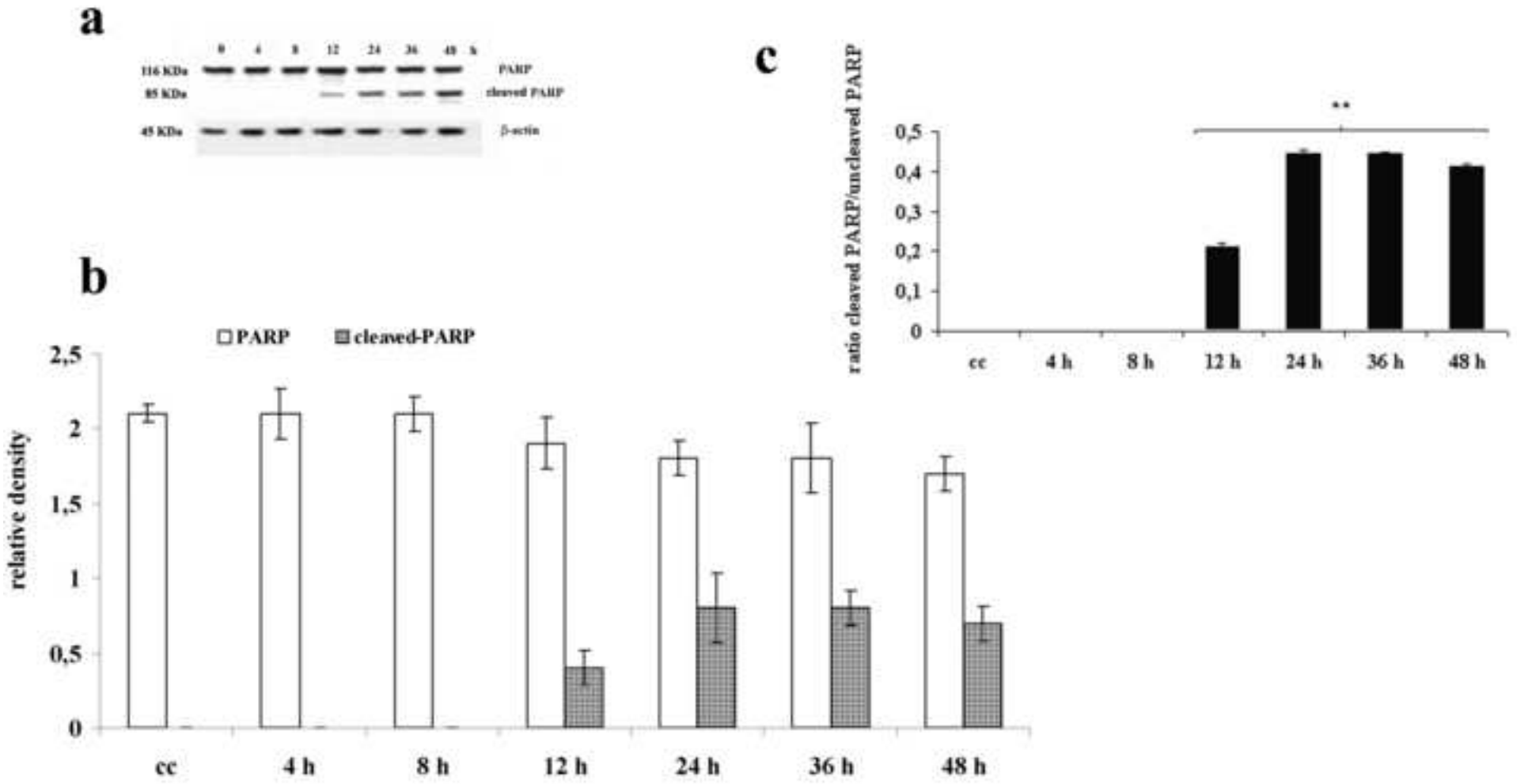
a
0 4 8 12 24 36 48 h
116 KDa
85 KDa
45 KDa
PARP
cleaved PARP
β-actin
b
PARP
cleaved-PARP
relative density
2,5
2
1,5
1
0,5
0
cc
4 h
8 h
12 h
24 h
36 h
48 h
c
ratio cleaved PARP/uncleaved PARP
0,5
0,4
0,3
0,2
0,1
0
**
cc
4 h
8 h
12 h
24 h
36 h
48 h

Figure 7

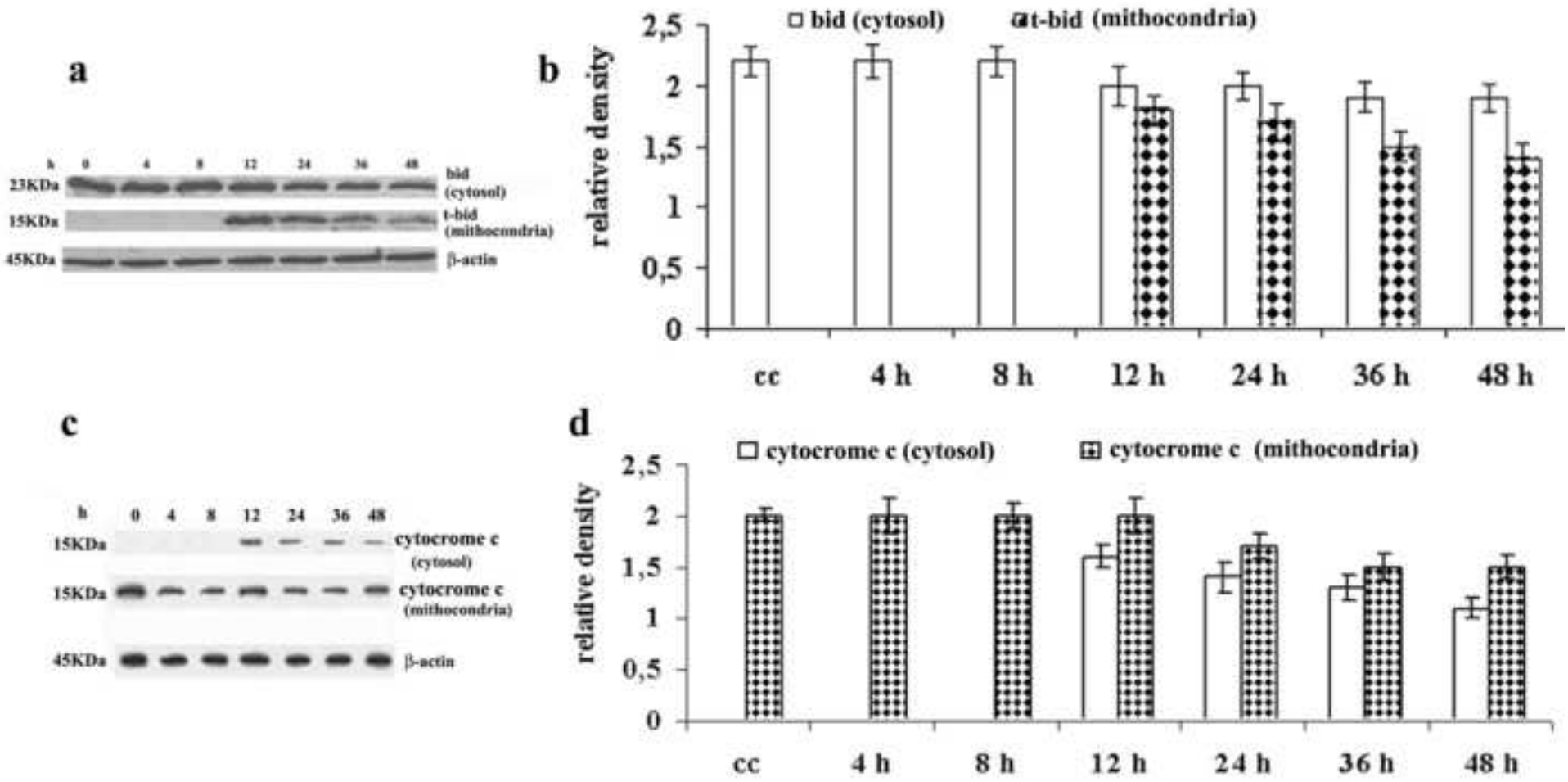
a
h 0 4 8 12 24 36 48
23KDa
bid (cytosol)
15KDa
t-bid (mithocondria)
45KDa
β-actin
b
bid (cytosol)
t-bid (mithocondria)
relative density
2,5
2
1,5
1
0,5
0
cc
4 h
8 h
12 h
24 h
36 h
48 h
c
h 0 4 8 12 24 36 48
15KDa
cytocrome c (cytosol)
15KDa
cytocrome c (mithocondria)
45KDa
β-actin
d
cytocrome c (cytosol)
cytocrome c (mithocondria)
relative density
2,5
2
1,5
1
0,5
0
cc
4 h
8 h
12 h
24 h
36 h
48 h

Figure 8

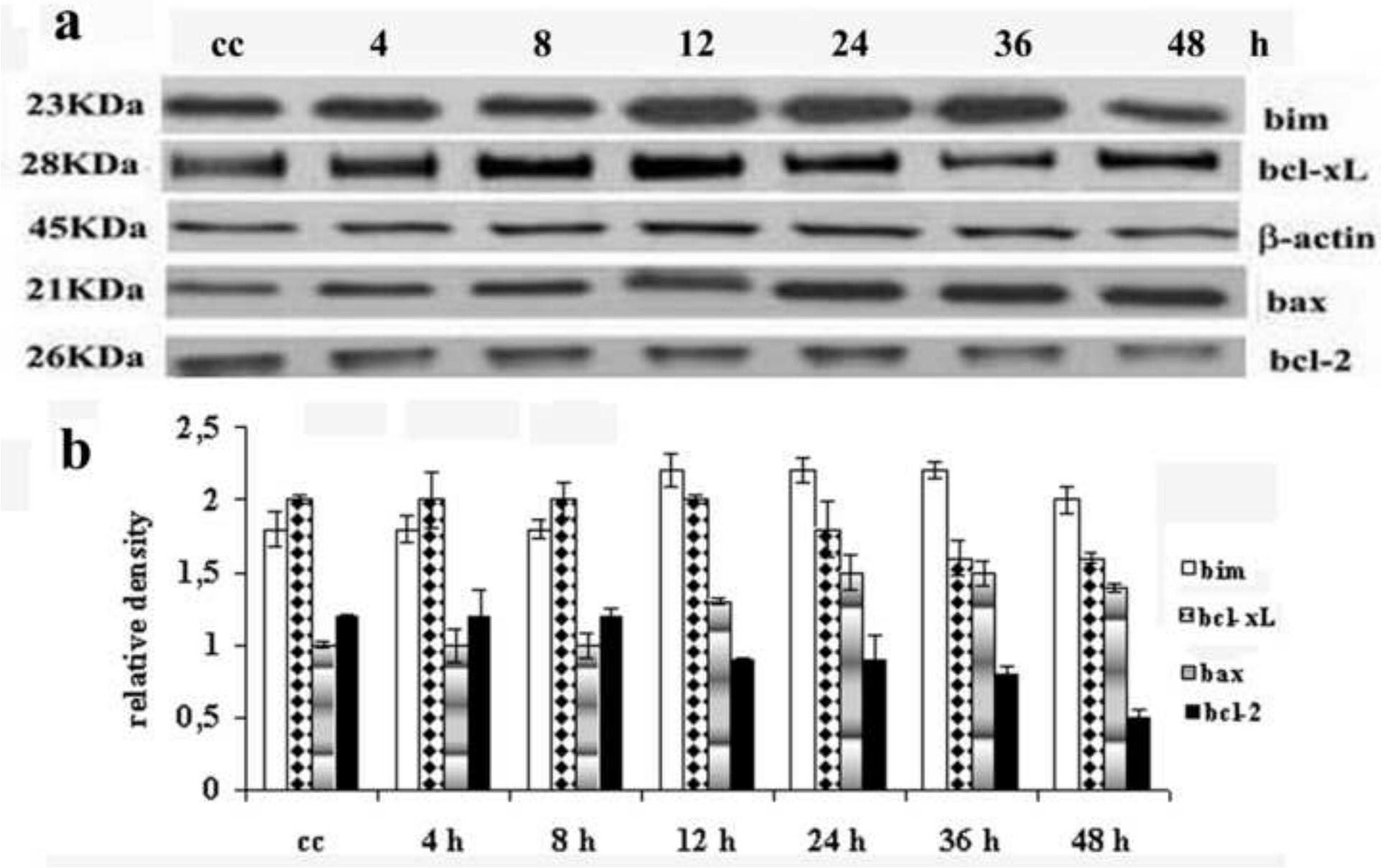
a
cc
4
8
12
24
36
48
h
23KDa
bim
28KDa
bcl-xL
45KDa
β-actin
21KDa
bax
26KDa
bcl-2
b
relative density
2,5
2
1,5
1
0,5
0
bim
bcl-xL
bax
bcl-2
cc
4 h
8 h
12 h
24 h
36 h
48 h